

High-density genetic mapping identifies new susceptibility loci for rheumatoid arthritis

Steve Eyre^{1,2,24}, John Bowes^{1,2,24}, Dorothee Diogo^{3-5,24}, Annette Lee⁶, Anne Barton^{1,2}, Paul Martin^{1,2}, Alexandra Zhernakova^{7,8}, Eli Stahl³⁻⁵, Sebastien Viatte^{1,2}, Kate McAllister^{1,2}, Christopher I Amos⁹, Leonid Padyukov¹⁰, Rene E M Toes⁷, Tom W J Huizinga⁷, Cisca Wijmenga⁸, Gosia Trynka^{3-5,8}, Lude Franke⁸, Harm-Jan Westra⁸, Lars Alfredsson¹¹, Xinli Hu^{3-5,12}, Cynthia Sandor³⁻⁵, Paul I W de Bakker^{3-5,13,14}, Sonia Davila¹⁵, Chiea Chuen Khor¹⁵, Khai Koon Heng¹⁵, Robert Andrews¹⁶, Sarah Edkins¹⁶, Sarah E Hunt¹⁶, Cordelia Langford¹⁶, Deborah Symmons^{1,2}, Biologics in Rheumatoid Arthritis Genetics and Genomics Study Syndicate¹⁷, Wellcome Trust Case Control Consortium¹⁷, Pat Concannon¹⁸, Suna Onengut-Gumuscu¹⁸, Stephen S Rich¹⁸, Panos Deloukas¹⁶, Miguel A Gonzalez-Gay¹⁹, Luis Rodriguez-Rodriguez²⁰, Lisbeth Ärlsetig^{21,22}, Javier Martin²³, Solbritt Rantapää-Dahlqvist^{21,22}, Robert M Plenge^{3-5,25}, Soumya Raychaudhuri^{1-5,25}, Lars Klareskog^{10,25}, Peter K Gregersen^{6,25} & Jane Worthington^{1,2,25}

Using the ImmunoChip custom SNP array, which was designed for dense genotyping of 186 loci identified through genome-wide association studies (GWAS), we analyzed 11,475 individuals with rheumatoid arthritis (cases) of European ancestry and 15,870 controls for 129,464 markers. We combined these data in a meta-analysis with GWAS data from additional independent cases ($n = 2,363$) and controls ($n = 17,872$). We identified 14 new susceptibility loci, 9 of which were associated with rheumatoid arthritis overall and five of which were specifically associated with disease that was positive for anticitrullinated peptide antibodies, bringing the number of confirmed rheumatoid arthritis risk loci in individuals of European ancestry to 46. We refined the peak of association to a single gene for 19 loci, identified secondary independent effects at 6 loci and identified association to low-frequency variants at 4 loci. Bioinformatic analyses generated strong hypotheses for the causal SNP at seven loci. This study illustrates the advantages of dense SNP mapping analysis to inform subsequent functional investigations.

Rheumatoid arthritis is a common, complex disease affecting up to 1% of the adult population. It is an archetypal autoimmune disease typified by the presence of serum autoantibodies, including antibodies directed against the Fc portion of immunoglobulins (rheumatoid factor) and against citrullinated peptides (anticitrullinated peptide antibodies (ACPAs)). Genetic studies of rheumatoid arthritis, including the recent application of GWAS, have identified 32 risk loci among individuals of European ancestry, including *HLA-DRB1*, *PTPN22* and other loci with shared autoimmune associations^{1,2}.

The ImmunoChip consortium was formed to design a custom Illumina Infinium array that leveraged the remarkable genetic overlap of susceptibility loci identified across a range of autoimmune diseases. The custom array allows investigators to perform gene-discovery and fine-mapping experiments in a coordinated manner. Full details of this array have been described previously³. Briefly, it consists of all known SNPs from the 1000 Genomes Project as well as private resequencing efforts for 186 loci known to be involved in any of 12 autoimmune diseases. For these loci, there is the unique opportunity to fine map associations to autoimmune diseases. Additional SNPs were included as part of a deep replication effort. This provided the opportunity not only to identify new rheumatoid arthritis associations with loci implicated in other autoimmune diseases or with variants showing suggestive statistical evidence for association from a previous meta-analysis but also to refine the GWAS signal and reduce the number of potential causal variants in the 31 confirmed non-*HLA* loci.

We tested 129,464 polymorphic markers passing quality control with a minor allele frequency (MAF) >1% in 11,475 cases (7,222 ACPA positive, 3,297 ACPA negative and 957 unassigned) and 15,870 controls (Table 1 and Supplementary Tables 1 and 2). We performed an analysis on the total rheumatoid arthritis dataset and also on subsets stratified by ACPA status (Supplementary Table 3). We also had access to GWAS data for an additional 2,363 ACPA-positive cases and 17,872 controls that were independent of the current study (Table 1). We found strong evidence of association for the previously identified susceptibility loci (Table 2 and Supplementary Tables 3 and 4).

We identified 14 new rheumatoid arthritis loci for populations of European ancestry (*TYK2*, *IRAK1*, *TLE3*, *RASGRP1*, *PADI4*, *IL6R*, *IRF8*, *ARID5B*, *IKZF3*, *RUNX1*, *POU3F1*, *RCAN1*, *CD5* and *GATA3*) at genome-wide levels of significance ($P < 5 \times 10^{-8}$) (Fig. 1), 7 with

A full list of affiliations appears at the end of the paper.

Received 10 May; accepted 10 October; published online 11 November 2012; doi:10.1038/ng.2462

Table 1 Sample collections

| Collection | Cases | | | | Controls | | |
|------------|---------------|------------|-------|-------|----------|------------|----|
| | All | Female (%) | ACPA+ | ACPA- | All | Female (%) | |
| ImmunoChip | UK | 3,870 | 74 | 2,406 | 1,000 | 8,430 | 53 |
| | Swedish EIRA | 2,762 | 70 | 1,762 | 987 | 1,940 | 73 |
| | United States | 2,536 | 75 | 1,803 | 593 | 2,134 | 65 |
| | Dutch | 648 | 66 | 330 | 301 | 2,004 | 42 |
| | Swedish Umea | 852 | 70 | 524 | 242 | 963 | 69 |
| | Spanish | 807 | 74 | 397 | 216 | 399 | 65 |
| | TOTAL | 11,475 | 73 | 7,222 | 3,339 | 15,870 | 57 |
| GWAS | BRASS (US) | 479 | 82 | 479 | – | 1,627 | 45 |
| | Canada | 586 | 76 | 586 | – | 1,553 | 54 |
| | NARAC2 (US) | 746 | 48 | 746 | – | 6,567 | 49 |
| | WTCCC (UK) | 552 | 74 | 552 | – | 8,125 | 46 |
| | TOTAL | 2,363 | 68 | 2,363 | – | 17,872 | 48 |
| TOTAL | 13,838 | 72 | 9,585 | 3,297 | 33,742 | 52 | |

Rheumatoid arthritis cases and controls for the ImmunoChip analysis were assembled from a number of different studies from six centers across five countries (Online Methods). Genotype data for additional samples analyzed in previously published rheumatoid arthritis ACPA-positive GWAS were available from four studies. Rheumatoid arthritis cases were classified as ACPA positive (ACPA+) or ACPA negative (ACPA-). Swedish EIRA, Swedish Epidemiological Investigation of Rheumatoid Arthritis; BRASS, Brigham and Women's Hospital Rheumatoid Arthritis Sequential Study; NARAC2, North American Rheumatoid Arthritis Consortium 2; WTCCC, Wellcome Trust Case Control Consortium.

ImmunoChip data alone (Table 2) and a further 7 when ImmunoChip data were combined with the GWAS meta-analysis data (Table 2). These loci add 4% to the estimate of heritability explained by confirmed loci, bringing the total to 51%, of which HLA explains 36%. When we removed all known loci from the ImmunoChip data, we still observed evidence of an excessive number of nominally associated alleles, which is consistent with the possibility that there are many additional undiscovered alleles⁴ (Supplementary Fig. 1). Notably, when we applied a study-wide significance threshold of $P < 9.0 \times 10^{-7}$ (calculated on the basis of the number of effective independent tests when accounting for linkage disequilibrium (LD)), we also found a significant association at two additional loci: *ELMO1* (rs75351767, $P_{\text{all}} = 2.94 \times 10^{-7}$) and *BACH2* (rs72928038, $P_{\text{all}} = 8.23 \times 10^{-7}$) (Supplementary Table 3). A further eight loci were implicated at suggestive levels of significance ($P < 1 \times 10^{-5}$) in either the full or the ACPA-positive subgroup analysis, including *PTPN22* (rs62097857, $P_{\text{all}} = 4.4 \times 10^{-6}$), *TNIP1* (rs6579837, $P_{\text{pos}} = 1.7 \times 10^{-6}$) and *TNFSF4* (rs61828284, $P_{\text{pos}} = 5.4 \times 10^{-6}$) (Supplementary Table 3).

Previously, we fine mapped MHC associations observed in GWAS data of partially overlapping samples by applying imputation of HLA classical alleles and amino acids⁵. The ImmunoChip platform includes denser SNP coverage within the MHC region, which facilitates more accurate imputation. In a preliminary analysis applying the same imputation and fine-mapping approach to ACPA-positive cases and controls typed on ImmunoChip, we observed the same associations that we reported previously. The most significant polymorphic nucleotide was again rs17878703, mapping to position 11 of the HLA-DRB1 peptide sequence ($P < 10^{-677}$). Testing individual amino acid positions within HLA-DRB1 revealed the strongest association to be at position 11 ($P < 10^{-745}$). Conditioning on the position 11 effect, we observed an association at position 71 ($P = 6 \times 10^{-60}$). Finally, conditioning on effects at both positions 11 and 71, we observed a significant association at position 74 ($P = 7 \times 10^{-19}$). Adjusting for all HLA-DRB1 alleles to identify independent effects outside this gene, we observed significant associations at HLA-B corresponding to the presence of aspartate at position 9 in the peptide sequence ($P = 1 \times 10^{-17}$). Adjusting for all HLA-DRB1 alleles and Asp9 in HLA-B, we observed associations

at HLA-DPB1 corresponding to the presence of phenylalanine at position 9 in the peptide sequence ($P = 1 \times 10^{-17}$).

Although it has been demonstrated that ACPA-positive disease and ACPA-negative disease have different allelic associations at the MHC and at *PTPN22* (ref. 6), previous studies have not been sufficiently powered to address this issue definitively in additional non-MHC loci. Here we analyzed 3,297 ACPA-negative cases and identified association at genome-wide significance to *ANKRD55* (rs71624119, $P = 5.2 \times 10^{-12}$, odds ratio (OR) = 0.78) in addition to *HLA* (rs4143332, $P = 2.9 \times 10^{-15}$, OR = 1.37) (Supplementary Table 3). Notably, *ANKRD55* has a similar effect in ACPA-negative as in ACPA-positive disease. Comparing the associations in the ACPA-positive and ACPA-negative subgroups, we observed that for the 45 non-*HLA* loci, around half showed a significantly larger effect size in ACPA-positive disease ($P < 0.05$ for the comparison of the ORs), with 5 of these loci having a markedly

stronger association with this form of disease (*PTPN22*, *CCR6*, *CD40*, *RASGRP1* and *TAGAP*). Eleven loci showed no statistical difference in association to either form of rheumatoid arthritis (Supplementary Table 5). This preliminary analysis indicates that differences in the serological subtype of disease may be reflected in a difference in genetic predisposition, potentially providing a basis for stratified medicine.

We found that the majority of the 14 loci newly associated with rheumatoid arthritis susceptibility, along with the previously confirmed loci, contain genes that are strongly linked to immune function using GRAIL analysis (Supplementary Table 6 and Supplementary Fig. 2), for example, *CD5*, *IRF8* and *TYK2*. We also report a new association with *IRAK1*, which has previously been associated with systemic lupus erythematosus⁷. This is the first association of the X chromosome locus with rheumatoid arthritis and is of relevance given the female predominance of both diseases (9:1 and 3:1 ratios of females to males in systemic lupus erythematosus and rheumatoid arthritis, respectively). Interestingly, this locus has been shown to occasionally escape X inactivation in female cells⁸. Three of the new loci confirmed here in samples of European ancestry have been previously associated with rheumatoid arthritis in either samples of east Asian ancestry (*PADI4* and *ARID5B*) or when using a multiethnic approach (*IKZF3*)^{9–11}. The SNPs associated in this study are moderately correlated with those identified in samples of east Asian origin (*PADI4* SNPs rs2240336 and rs766449, $r^2 = 0.25$, $D' = 1$; *ARID5B* SNPs rs12764378 and rs10821944, $r^2 = 0.52$, $D' = 0.86$). *PADI* genes are involved in the citrullination of peptides and, as such, are strong candidates for involvement in disease given the presence of ACPA autoantibodies. Although the association at *PADI4* (rs2240336) is greater in ACPA-positive (OR = 0.88, $P = 6.49 \times 10^{-9}$) compared to ACPA-negative cases (OR = 0.93, $P = 0.01$), our formal test comparing the ORs between these subgroups did not show a statistically significant difference ($P = 0.14$).

We applied conditional logistic regression to test for secondary effects within each locus. In six non-*HLA* loci (13%) (*TNFAIP3*, *CD28*, *REL*, *STAT4*, *TYK2* and *RASGRP1*), we found additional independent association signals (Supplementary Fig. 3). In total, we observed 51 independent risk alleles in 45 non-*HLA* rheumatoid arthritis loci. To test the possibility that the two risk alleles tag an untyped SNP,

Table 2 Non-*HLA* loci associated with rheumatoid arthritis at a genome-wide significance level

| SNP | Gene | Chr. | MAF | Risk allele | <i>P</i> | OR | LD region $r^2 > 0.9^a$ | Region size (kb) | Localization of LD region ($r^2 > 0.9$) relative to nearest genes |
|---|---------------------------|-------|------|-------------|-----------------------|------|-------------------------|------------------|--|
| New loci identified through Immunochip analyses | | | | | | | | | |
| rs34536443 ^b | <i>TYK2</i> | 19p13 | 0.04 | G | 2.3×10^{-14} | 0.62 | 10,427,721–10,492,274 | 64.55 | 47.96 kb 5' to exon 13 of <i>RAVER1</i> ; complete <i>ICAM3</i> ; complete <i>TYK2</i> |
| rs13397 ^b | <i>IRAK1</i> | Xq28 | 0.12 | A | 1.2×10^{-12} | 1.27 | 153,196,345–153,248,248 | 51.9 | 5' to exon 2 of <i>TMEM187</i> ; <i>HCFC1</i> ; 25 kb 3' of <i>IRAK1</i> |
| rs8026898 ^b | <i>TLE3^c</i> | 15q23 | 0.29 | A | 1.4×10^{-10} | 1.17 | 69,984,462–70,010,647 | 26.19 | 329.48 kb 3' of <i>TLE3</i> |
| rs8043085 ^b | <i>RASGRP1</i> | 15q14 | 0.25 | A | 1.4×10^{-10} | 1.17 | 38,828,140–38,844,106 | 15.97 | Intron 2 of <i>RASGRP1</i> |
| rs2240336 ^b | <i>PADI4</i> | 1p36 | 0.42 | A | 5.9×10^{-9} | 0.88 | 17,673,102–17,674,402 | 1.30 | Intron 9 of <i>PADI4</i> |
| rs8192284 ^d (rs2228145) | <i>IL6R</i> | 1q21 | 0.42 | C | 1.3×10^{-8} | 0.90 | 154,418,749–154,428,283 | 9.54 | Introns 6–9 of <i>IL6R</i> |
| rs13330176 ^b | <i>IRF8</i> | 16q24 | 0.22 | A | 4.0×10^{-8} | 1.15 | 86,016,026–86,019,087 | 3.06 | 59.83 kb 3' of <i>IRF8</i> |
| New loci identified through joint analyses of Immunochip and GWAS data | | | | | | | | | |
| rs12764378 ^e | <i>ARID5B^c</i> | 10q21 | 0.23 | A | 4.5×10^{-10} | 1.14 | 63,786,554–63,800,004 | 13.45 | Intron 4 of <i>ARID5B</i> |
| rs9979383 ^f | <i>RUNX1^c</i> | 21q22 | 0.36 | G | 5.0×10^{-10} | 0.90 | 36,712,588–36,715,761 | 3.17 | 5' region of <i>RUNX1</i> |
| rs12936409/ rs2872507 ^f | <i>IKZF3</i> | 17q12 | 0.47 | A | 2.8×10^{-9} | 1.10 | 37,912,377–38,080,912 | 168.54 | <i>IKZF3</i> ; <i>GSDMB</i> ; intron 1 to 164.92 kb 3' of <i>ORMDL3</i> |
| rs883220 ^e | <i>POU3F1^c</i> | 1p34 | 0.26 | A | 2.1×10^{-8} | 0.89 | 38,614,867–38,644,861 | 30.00 | 102.42 kb 5' of <i>POU3F1</i> |
| rs2834512 ^e | <i>RCAN1^c</i> | 21q22 | 0.12 | A | 2.1×10^{-8} | 0.86 | 35,909,625–35,930,915 | 21.29 | Intron 1 of <i>RCAN1</i> |
| rs595158 ^f | <i>CD5</i> | 11q12 | 0.49 | C | 3.4×10^{-8} | 1.09 | 60,888,001–60,922,634 | 34.63 | Intron 5 to 27.31 kb 3' of <i>CD5</i> ; intron 1 to 9.73 kb 3' of <i>VPS37C</i> |
| rs2275806 ^e | <i>GATA3^c</i> | 10p14 | 0.41 | G | 4.6×10^{-8} | 1.11 | 8,095,340–8,097,368 | 2.03 | 227 bp 5' to exon 2 of <i>GATA3</i> |
| Results for known loci on Immunochip | | | | | | | | | |
| rs2476601 ^b | <i>PTPN22</i> | 1p13 | 0.09 | A | 7.5×10^{-77} | 1.78 | 114,303,808–114,377,568 | 73.76 | Complete <i>RSBN1</i> ; exon 14 to 52.62 kb 3' of <i>PTPN22</i> |
| rs71624119 ^d | <i>ANKRD55</i> | 5q11 | 0.25 | A | 5.6×10^{-20} | 0.81 | 55,440,730–55,442,249 | 1.52 | Intron 6 of <i>ANKRD55</i> |
| rs6920220 ^b | <i>TNFAIP3</i> | 6q23 | 0.20 | A | 2.3×10^{-13} | 1.20 | 137,959,235–138,006,504 | 47.27 | 181.85 kb 5' of <i>TNFAIP3</i> |
| rs932036 ^d | <i>RBPJ</i> | 4p15 | 0.30 | A | 2.0×10^{-10} | 1.14 | 26,085,480–26,128,710 | 43.23 | 36.37 kb 5' of <i>RBPJ</i> |
| rs59466457 ^b | <i>CCR6</i> | 6q27 | 0.44 | A | 2.7×10^{-10} | 1.15 | 167,526,096–167,540,842 | 14.75 | Intron 1 of <i>CCR6</i> |
| rs13426947 ^d | <i>STAT4</i> | 2q32 | 0.19 | A | 7.2×10^{-10} | 1.15 | 191,900,449–191,935,804 | 35.36 | Intron 5 to 18 of <i>STAT4</i> |
| rs2812378 ^b | <i>CCL21</i> | 9p13 | 0.34 | G | 7.2×10^{-10} | 1.15 | 34,707,373–34,710,338 | 2.97 | <i>CCL21</i> |
| rs6032662 ^b | <i>CD40</i> | 20q13 | 0.24 | G | 1.4×10^{-9} | 0.86 | 44,730,245–44,747,947 | 17.70 | 16.67 kb 5' to intron 1 of <i>CD40</i> |
| rs2843401 ^b | <i>MMEL1</i> | 1p36 | 0.33 | A | 6.6×10^{-9} | 0.87 | 2,516,781–2,709,164 | 192.38 | Complete <i>MMEL1</i> ; <i>C10RF93</i> ; <i>TTC34</i> |
| rs10209110 ^d | <i>AFF3</i> | 2q11 | 0.49 | A | 1.1×10^{-8} | 0.90 | 100,640,432–100,730,111 | 89.68 | 5' region to intron 2 of <i>AFF3</i> |
| rs34695944 ^b | <i>REL</i> | 2p16 | 0.37 | G | 2.6×10^{-8} | 1.13 | 61,072,664–61,164,331 | 91.67 | Complete <i>REL</i> |
| rs11571302 ^b | <i>CTLA4</i> | 2q33 | 0.48 | A | 4.5×10^{-8} | 0.89 | 204,738,919–204,745,003 | 6.08 | 236 bp 3' of <i>CTLA4</i> ; 56.47 kb 5' of <i>ICOS</i> |
| rs39984 ^d | <i>GIN1</i> | 5q21 | 0.32 | A | 9.3×10^{-8} | 0.88 | 102,595,778–102,625,335 | 29.56 | Intron 1 to 10.97 kb 3' of <i>C5orf30</i> ; 139.92 kb 5' of <i>GIN1</i> |
| rs35677470 ^d | <i>DNASE1L3</i> | 3p14 | 0.08 | A | 1.7×10^{-7} | 1.19 | 58,181,499–58,183,636 | 2.14 | Exon 8 to intron 9 of <i>DNASE1L3</i> ; 134.97 kb 5' of <i>PXK</i> |
| rs3807306 ^b | <i>IRF5</i> | 7q32 | 0.49 | C | 1.9×10^{-7} | 0.89 | 128,580,680–128,580,680 | 1 bp | Intron 1 of <i>IRF5</i> |
| rs3218251 ^b | <i>IL2RB</i> | 22q12 | 0.25 | A | 1.9×10^{-7} | 1.13 | 37,544,245–37,545,505 | 1.26 | Intron 1 of <i>IL2RB</i> |
| rs4938573 ^b | <i>DDX6</i> | 11q23 | 0.18 | G | 5.3×10^{-7} | 0.87 | 118,662,993–118,745,884 | 82.89 | Complete <i>SETP16</i> ; 1.14 kb 5' of <i>DDX6</i> |
| rs6546146 ^b | <i>SPRED2</i> | 2p14 | 0.38 | A | 8.0×10^{-7} | 0.90 | 65,556,324–65,598,300 | 41.98 | Introns 1–4 of <i>SPRED2</i> |
| rs629326 ^b | <i>TAGAP</i> | 6q25 | 0.41 | C | 1.1×10^{-6} | 0.90 | 159,489,791–159,496,713 | 6.92 | 23.61 kb 5' of <i>TAGAP</i> |
| rs10739580 ^b | <i>TRAF1</i> | 9q33 | 0.33 | G | 1.7×10^{-6} | 1.12 | 123,640,500–123,708,286 | 67.79 | Complete <i>TRAF1</i> |
| rs10795791 ^d | <i>IL2RA</i> | 10p15 | 0.40 | G | 3.0×10^{-6} | 1.09 | 6,106,266–6,108,340 | 2.08 | 1.93 kb 5' of <i>IL2RA</i> |
| rs4840565 ^d | <i>BLK</i> | 8p23 | 0.27 | G | 3.9×10^{-6} | 1.10 | 11,338,383–11,352,485 | 14.10 | 13.13 kb 5' to intron 1 of <i>BLK</i> |
| rs798000 ^b | <i>CD2</i> | 1p13 | 0.34 | G | 6.2×10^{-6} | 1.11 | 117,280,696–117,280,696 | 1 bp | 16.31 kb 5' of <i>CD2</i> |
| rs1980422 ^f | <i>CD28</i> | 2q33 | 0.23 | G | 8.7×10^{-6} | 1.12 | 204,610,004–204,634,569 | 24.57 | 7.45 kb 3' of <i>CD28</i> ; 97.94 kb 5' of <i>CTLA4</i> |
| rs2014863 ^d | <i>PTPRC</i> | 1q31 | 0.36 | C | 2.1×10^{-5} | 1.09 | 198,791,907–198,810,008 | 18.10 | 65.36 kb 3' of <i>PTPRC</i> |
| rs10683701 ^b | <i>KIF5A</i> | 12q13 | 0.33 | – | 2.3×10^{-5} | 0.90 | 58,034,835–58,105,094 | 70.26 | snoU13; 52.90 kb 5' to intron 5 of <i>OS9</i> ; 54.42 kb 3' of <i>KIF5A</i> |
| rs947474 ^d | <i>PRKCQ</i> | 10p15 | 0.17 | G | 2.5×10^{-5} | 0.90 | 6,390,450–6,390,450 | 1 bp | 78.66 kb 3' of <i>PRKCQ</i> |
| rs10494360 ^b | <i>FCGR2A</i> | 1q23 | 0.12 | G | 3.0×10^{-5} | 1.14 | 161,463,876–161,480,649 | 16.77 | 11.34 kb 5' to exon 5 of <i>FCGR2A</i> |
| rs6911690 ^b | <i>PRDM1</i> | 6q21 | 0.12 | G | 1.2×10^{-4} | 0.87 | 106,435,981–106,508,640 | 72.66 | 25.55 kb 5' of <i>PRDM1</i> |
| rs78560100 ^d | <i>IL2-IL21</i> | 4q27 | 0.07 | C | 5.8×10^{-4} | 1.13 | 123,030,583–123,503,591 | 473.01 | <i>KIAA1109</i> ; <i>ADAD1</i> ; <i>IL2</i> ; 30.19 kb 3' of <i>IL21</i> |
| rs570676 ^b | <i>TRAF6</i> | 11p12 | 0.38 | A | 2.1×10^{-3} | 0.93 | 36,486,064–36,519,624 | 33.56 | Intron 3 to 22.51 kb 3' of <i>TRAF6</i> |

Newly identified loci are shown with either the best SNP on Immunochip (first tier), if $P < 5 \times 10^{-8}$, or the most associated SNP from the combined analysis of GWAS and Immunochip data (second tier). Previously identified loci are shown with the most significantly associated SNP on Immunochip (bottom tier).

^aCoordinates are based on the GRCh37 assembly. ^bData from Immunochip for ACPA-positive individuals. ^cRegion not included for dense mapping on Immunochip. ^dData are from all rheumatoid arthritis samples on Immunochip. ^eResults from adding ACPA-positive Immunochip and GWAS data. ^fResults from adding GWAS samples and all rheumatoid arthritis Immunochip data. Chr., chromosome.

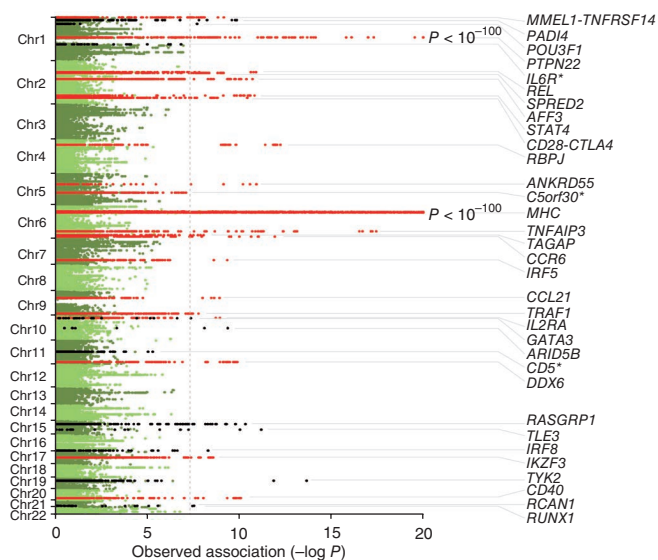


Figure 1 Manhattan plot of association statistics highlighting all autosomal loci associated with rheumatoid arthritis in this study. The P values of association to ACPA-positive rheumatoid arthritis from the meta-analysis of the Immunochip and GWAS data are shown. Known and newly identified rheumatoid arthritis risk loci are shown in red and black, respectively. Three associated loci (identified by asterisks) only reach $P < 5 \times 10^{-8}$ when both ACPA-positive and ACPA-negative cases are included in the analysis. The dashed gray line indicates genome-wide significance ($P = 5 \times 10^{-8}$).

we carried out a haplotype analysis of the six loci but found no evidence for haplotype-specific effects at any locus (**Supplementary Table 7**). At only four loci (*REL*, *CD28*, *TYK2* and *TNFAIP3*) did we observe associations with low-frequency variants ($MAF < 0.05$) (**Supplementary Table 8**).

Out of the 46 rheumatoid arthritis susceptibility loci, 39 were densely genotyped by Immunochip. For 12 loci, we observed that the most strongly associated SNP was not tightly linked to the previously reported lead SNP at that locus, shifting the association signal (**Supplementary Table 9**). For the 39 confirmed non-*HLA* rheumatoid arthritis loci on Immunochip, dense mapping refined the association to a single gene for 19 loci (**Supplementary Table 10**).

Our analysis also identified seven nonsynonymous SNPs within exonic regions (**Table 3**), as well as a number showing strong regulatory potential (**Supplementary Table 11**), that are highly correlated ($r^2 > 0.9$) with the lead SNP and are strong candidates for the etiological variant. The most strongly associated SNP at the *IL6R* locus (rs8192284) is nonsynonymous, shows high correlation with circulating IL-6R concentrations and, as well as being associated with a

decrease risk of coronary heart disease^{12,13}, is in strong LD ($r^2 = 0.97$, $D' = 1$) with a SNP recently reported to be associated with asthma (rs4129267)¹⁴. Notably, the risk allele at the asthma-associated SNP ($OR = 1.09$, $P = 2.4 \times 10^{-8}$) is protective for rheumatoid arthritis ($OR = 0.9$, $P = 1.3 \times 10^{-8}$). IL-6R is the target of the biologic drug tocilizumab, which has been shown to be an effective treatment for rheumatoid arthritis. Abatacept is another biologic drug with therapeutic efficacy in clinical trials that targets another rheumatoid arthritis susceptibility gene, *CTLA4*. These examples highlight the potential for targeting genes within risk loci.

Testing for statistical interactions between the 46 lead SNPs in confirmed rheumatoid arthritis loci identified preliminary evidence for six significant pairwise interactions after Bonferroni correction ($P < 5 \times 10^{-4}$) (**Supplementary Table 12**). The *GATA3-PRKCCQ* interaction is supported by earlier biological observations¹⁵.

Among 38 rheumatoid arthritis-associated SNPs or proxies accessed for expression quantitative trait loci (eQTL) analysis, 18 showed an eQTL effect on at least one probe, giving a total of 51 SNP-probe combinations with a significant eQTL effect (**Supplementary Table 13**). Among these 18 SNPs, 11 showed an independent or primary eQTL effect on one or more probes (20 SNP-probe combinations), whereas seven SNPs were not significant after conditioning the strongest eQTL signal in the locus.

Using a previously described approach, we assessed whether the 46 independent rheumatoid arthritis-associated regions, defined by previously known and newly discovered SNP associations, harbored genes that were specifically expressed in distinct immune cell types¹⁶. We found in a large expression dataset of 223 sorted mouse immune cells¹⁷ that these regions contained genes that were most significantly more specifically expressed in $CD4^+$ effector memory T-cell subsets ($P < 10^{-7}$) (**Supplementary Fig. 4**).

Of the diseases sharing susceptibility loci with rheumatoid arthritis, systematic fine mapping has only been published so far for celiac disease³. Previously, the two diseases were found to share six confirmed non-*HLA* loci (*MMEL*, *REL*, *CD28-CTLA4*, *TNFAIP3*, *TAGAP* and *IL2-IL21*)². Immunochip data now identifies an additional four confirmed loci common to both diseases (*DDX6*, *STAT4*, *PRKCCQ* and *IRAK1*) and a further four potential rheumatoid arthritis loci (*BACH2*, $P = 8.2 \times 10^{-7}$; *ELMO1*, $P = 2.9 \times 10^{-7}$; *PTPN22*, $P = 4.4 \times 10^{-6}$; and *PVT1*, $P = 2 \times 10^{-5}$) in common with confirmed celiac disease loci (**Supplementary Table 14**). Of the ten shared rheumatoid arthritis and celiac disease loci, four have the same lead SNP (*CD28*, *IL2-IL21*, *TNFAIP3* and *IRAK1*) and a fifth (*MMEL1*) shares highly correlated SNPs ($r^2 > 0.88$), and for all of these variants, the risk allele is the same for both diseases. For two loci (*PRKCCQ* and *DDX6*), the lead SNPs are only moderately correlated ($r^2 > 0.62$), with the minor allele being protective in both diseases. The effects in *STAT4* seem quite different, with three independent effects in celiac disease and two different independent associations in rheumatoid

Table 3 Potentially causal exonic SNPs located by Immunochip dense genotyping

| Chr. | Position | Gene | SNP | MAF | r^2 with lead | SNP location | Allele | Amino acid change | PolyPhen | SIFT | Conservation |
|------|-------------|-----------------|------------|------|-----------------|--------------------------------------|--------|-------------------|-------------------|-------------|--------------|
| 1 | 2,535,613 | <i>MMEL1</i> | rs4648562 | 0.33 | 1 | Essential splice site | A | – | – | – | 1 |
| 1 | 114,377,568 | <i>PTPN22</i> | rs2476601 | 0.12 | Lead | Nonsynonymous coding | A | p.Arg620Trp | Benign | Tolerated | 0.992 |
| 1 | 154,426,970 | <i>IL6R</i> | rs2228145 | 0.38 | Lead | Nonsynonymous coding | C | p.Asp358Ala | Benign | Tolerated | 0.008 |
| 3 | 58,183,636 | <i>DNASE1L3</i> | rs35677470 | 0.09 | Lead | Nonsynonymous coding | A | p.Arg206Cys | Probably damaging | Deleterious | 0.992 |
| 11 | 60,893,235 | <i>CD5</i> | rs2229177 | 0.47 | 0.96 | Nonsynonymous coding | C | p.Ala471Val | Probably damaging | Deleterious | 0.835 |
| 19 | 10,449,358 | <i>ICAM3</i> | rs7258015 | 0.23 | 1 | Nonsynonymous coding and splice site | C | p.Arg115Gly | Benign | Tolerated | 0 |
| 19 | 10,463,118 | <i>TYK2</i> | rs34536443 | 0.04 | Lead | Nonsynonymous coding | G | p.Pro1104Ala | Probably damaging | Deleterious | 0.189 |

Conservation is by phastCons17way; the study 99th percentile was 0.998, and the 95th percentile was 0.367. An essential splice site is a splice donor variant within the 2-bp region at the 5' end of an intron. A splice site is a sequence variant within 1–3 bp of the exon or 3–8 bp of the intron. Chr., chromosome.

arthritis. The strongest association signal for risk of celiac disease at TAGAP is with the minor allele of a SNP (rs182429) in moderate LD ($r^2 = 0.44$) with the rheumatoid arthritis risk SNP (rs629326). Indeed, when considering overlap of rheumatoid arthritis susceptibility loci with those of other autoimmune diseases, only the *PADI4* and *CCL21* non-MHC loci show unique association, suggesting that they may be important in determining that the autoimmune reaction is directed at synovial joints.

In summary, through fine mapping on a custom-made array designed to capture variation across a number of loci associated with autoimmune diseases, we have identified 14 new rheumatoid arthritis susceptibility loci in individuals of European ancestry, refined the peak of association to a single gene at 19 loci, identified 7 SNPs that might potentially be functional, found independent effects at 6 loci and detected association with SNPs with low MAF (<0.05) at four loci. In one-third of cases, imputation of GWAS signals without fine mapping would have implicated a different genetic region as being causal, thus illustrating the importance of dense fine-mapping analysis before embarking on intensive functional studies.

METHODS

Methods and any associated references are available in the [online version of the paper](#).

Note: Supplementary information is available in the [online version of the paper](#).

ACKNOWLEDGMENTS

We thank J. Barrett and C. Wallace for the SNP selection. We thank the Wellcome Trust Sanger Institute Genotyping Facility, and, in particular, E. Gray, S. Bumpstead, D. Simpkin and H. Blackburn. Genotyping of the UK Rheumatoid Arthritis Genetics samples was supported by the Arthritis Research UK grant reference number 17552 and the Manchester Biomedical Research Centre. This work was made possible by funds from the Arthritis Foundation (S.R., principal investigator) and the US National Institutes Health (K08AR055688 to S.R. and 1R01AR062886-01 to P.I.W.d.B.). P. Gilbert prepared the UK samples. Genotyping of the Swedish Umea samples was performed by the SNP&SEQ Technology Platform in Uppsala, which is supported by Uppsala University, Uppsala University Hospital, Science for Life Laboratory–Uppsala and the Swedish Research Council (contracts 80576801 and 70374401). This work was partially supported by the Redes Temáticas de Investigación Cooperativa en Salud (RETICS) Program, RD08/0075 (RIER), from the Instituto de Salud Carlos III, Spain. We acknowledge use of DNA from the UK Blood Services collection of Common Controls (UKBS-CC collection), which is funded by Wellcome Trust grant 076113/C/04/Z and by the US National Institutes for Health research program grant to the National Health Service Blood and Transplant (RP-PG-0310-1002). We acknowledge the use of DNA from the British 1958 Birth Cohort collection, which is funded by the UK Medical Research Council grant G0000934 and the Wellcome Trust grant 068545/Z/02. The North American Rheumatoid Arthritis Consortium and analysis of other US patient and control collections at the Feinstein Institute were supported by the US National Institutes of Health RO1-AR-4-4422, NO1-AR-2-2263; NO1-AR1-2256, RO1 AI068759 and RC2AR059092-01, with additional support from the Eileen Ludwig

Greenland Center for Rheumatoid Arthritis and the family of Robert S. Boas. R.M.P. is supported by grants from the US National Institutes of Health (R01-AR057108, R01-AR056768, U01-GM092691 and R01-AR059648) and holds a Career Award for Medical Scientists from the Burroughs Wellcome Fund.

AUTHOR CONTRIBUTIONS

J.W., P.K.G., L.K., S.R., R.M.P. and S. Eyre led the study. S. Eyre, J.B., J.W., R.M.P. and S.R. wrote the paper. J.B., E.S., S.V., A.Z., P.M., P.I.W.d.B., C.I.A., K.M. and D.D. performed the data and statistical analyses. A.L., A.B., L.P., R.E.M.T., T.W.J.H., C.W., G.T., L.F., H.-J.W., L.A., X.H., C.S., S.D., C.C.K., K.K.H., R.A., S. Edkins, S.E.H., C.L., D.S., P.C., S.O.-G., S.S.R., P.D., M.A.G.-G., L.R.-R., L.Á., J.M. and S.R.-D. contributed primarily to the patient ascertainment, sample collection and/or genotyping. All authors reviewed the final manuscript.

COMPETING FINANCIAL INTERESTS

The authors declare no competing financial interests.

Published online at <http://www.nature.com/doi/10.1038/ng.2462>.

Reprints and permissions information is available online at <http://www.nature.com/reprints/index.html>.

1. Stahl, E.A. *et al.* Genome-wide association study meta-analysis identifies seven new rheumatoid arthritis risk loci. *Nat. Genet.* **42**, 508–514 (2010).
2. Zhernakova, A. *et al.* Meta-analysis of genome-wide association studies in celiac disease and rheumatoid arthritis identifies fourteen non-HLA shared loci. *PLoS Genet.* **7**, e1002004 (2011).
3. Trynka, G. *et al.* Dense genotyping identifies and localizes multiple common and rare variant association signals in celiac disease. *Nat. Genet.* **43**, 1193–1201 (2011).
4. Stahl, E.A. *et al.* Bayesian inference analyses of the polygenic architecture of rheumatoid arthritis. *Nat. Genet.* **44**, 483–489 (2012).
5. Raychaudhuri, S. *et al.* Five amino acids in three HLA proteins explain most of the association between MHC and seropositive rheumatoid arthritis. *Nat. Genet.* **44**, 291–296 (2012).
6. Padyukov, L. *et al.* A genome-wide association study suggests contrasting associations in ACPA-positive versus ACPA-negative rheumatoid arthritis. *Ann. Rheum. Dis.* **70**, 259–265 (2011).
7. Jacob, C.O. *et al.* Identification of *IRAK1* as a risk gene with critical role in the pathogenesis of systemic lupus erythematosus. *Proc. Natl. Acad. Sci. USA* **106**, 6256–6261 (2009).
8. Carrel, L. & Willard, H.F. X-inactivation profile reveals extensive variability in X-linked gene expression in females. *Nature* **434**, 400–404 (2005).
9. Suzuki, A. *et al.* Functional haplotypes of *PADI4*, encoding citrullinating enzyme peptidylarginine deiminase 4, are associated with rheumatoid arthritis. *Nat. Genet.* **34**, 395–402 (2003).
10. Kurreeman, F.A. *et al.* Use of a multiethnic approach to identify rheumatoid-arthritis-susceptibility loci, 1p36 and 17q12. *Am. J. Hum. Genet.* **90**, 524–532 (2012).
11. Okada, Y. *et al.* Meta-analysis identifies nine new loci associated with rheumatoid arthritis in the Japanese population. *Nat. Genet.* **44**, 511–516 (2012).
12. Hingorani, A.D. & Casas, J.P. The interleukin-6 receptor as a target for prevention of coronary heart disease: a mendelian randomisation analysis. *Lancet* **379**, 1214–1224 (2012).
13. Sarwar, N. *et al.* Interleukin-6 receptor pathways in coronary heart disease: a collaborative meta-analysis of 82 studies. *Lancet* **379**, 1205–1213 (2012).
14. Ferreira, M.A. *et al.* Identification of *IL6R* and chromosome 11q13.5 as risk loci for asthma. *Lancet* **378**, 1006–1014 (2011).
15. Stevens, L. *et al.* Involvement of GATA3 in protein kinase C θ -induced Th2 cytokine expression. *Eur. J. Immunol.* **36**, 3305–3314 (2006).
16. Hu, X. *et al.* Integrating autoimmune risk loci with gene-expression data identifies specific pathogenic immune cell subsets. *Am. J. Hum. Genet.* **89**, 496–506 (2011).
17. Heng, T.S. & Painter, M.W. The Immunological Genome Project: networks of gene expression in immune cells. *Nat. Immunol.* **9**, 1091–1094 (2008).

¹Arthritis Research UK Epidemiology Unit, Centre for Musculoskeletal Research, University of Manchester, Manchester Academic Health Science Centre, Manchester, UK. ²National Institute for Health Research, Manchester Musculoskeletal Biomedical Research Unit, Central Manchester University Hospitals National Health Service Foundation Trust, Manchester Academic Health Sciences Centre, Manchester, UK. ³Division of Rheumatology, Immunology and Allergy, Brigham and Women's Hospital, Harvard Medical School, Boston, Massachusetts, USA. ⁴Division of Genetics, Brigham and Women's Hospital, Harvard Medical School, Boston, Massachusetts, USA. ⁵Program in Medical and Population Genetics, Broad Institute, Cambridge, Massachusetts, USA. ⁶The Feinstein Institute for Medical Research, North Shore–Long Island Jewish Health System, Manhasset, New York, USA. ⁷Department of Rheumatology, Leiden University Medical Centre, Leiden, The Netherlands. ⁸Department of Genetics, University Medical Center Groningen and University of Groningen, Groningen, The Netherlands. ⁹University of Texas MD Anderson Cancer Center, Houston, Texas, USA. ¹⁰Rheumatology Unit, Department of Medicine, Karolinska Institutet and Karolinska University Hospital Solna, Stockholm, Sweden. ¹¹Department of Environmental Medicine, Karolinska Institutet, Stockholm, Sweden. ¹²Harvard–Massachusetts Institute of Technology Division of Health Sciences and Technology, Boston, Massachusetts, USA. ¹³Department of Epidemiology, University Medical Center Utrecht, Utrecht, The Netherlands. ¹⁴Department of Medical Genetics, University Medical Center Utrecht, Utrecht, The Netherlands. ¹⁵Division of Human Genetics, Genome Institute of Singapore, Singapore. ¹⁶The Wellcome Trust Sanger Institute, Cambridge, UK. ¹⁷A list of members is provided in the **Supplementary Note**. ¹⁸Center for Public Health Genomics, University of Virginia, Charlottesville, Virginia, USA. ¹⁹Department of Rheumatology, Hospital Marques de Valdecilla, Instituto de Fundación e Investigación Marqués de Valdecilla, Santander, Spain. ²⁰Hospital Clínico San Carlos, Madrid, Spain. ²¹Department of Public Health and Clinical Medicine, Umeå University, Umeå, Sweden. ²²Department of Rheumatology, Umeå University, Umeå, Sweden. ²³EI Instituto de Parasitología y Biomedicina 'López-Neyra'-Consejo Superior de Investigaciones Científicas, Avenida del Conocimiento s/n, Granada, Spain. ²⁴These authors contributed equally to this work. ²⁵These authors jointly directed this work. Correspondence should be addressed to J.W. (jane.worthington@manchester.ac.uk).

ONLINE METHODS

Genotyping. All samples were genotyped for the Immunochip custom array in accordance with Illumina protocols at six centres: Sanger Centre, Hinxton, Cambridge, UK and the University of Virginia, USA (UK samples), Feinstein Institute, New York, USA (US and Spain samples), The Genome Institute, Singapore (Sweden EIRA samples), Department of Medical Sciences, SNP&SEQ Technology Platform, Uppsala University Hospital, Uppsala, Sweden (Sweden Umea samples) and Department of Genetics, University Medical Centre Groningen (The Netherlands samples).

Genotype calling and quality control. Genotype calling was performed on all samples at the University of Manchester as a single project using the Genotyping Module (v1.8.4) of the GenomeStudio Data Analysis software package. Initial genotype clustering was performed using the default Illumina cluster file (Immunochip_Gentrain_June2010.egt) and manifest file Immuno_BeadChip_11419691_B.bpm (NCBI build 36) using the GenTrain2 clustering algorithm. Poor-performing samples (call rate <0.90), labeled duplicates (selection informed by a tenth percentile GenCall score (p10 GC)) and samples identified after genotyping as inappropriate for inclusion were also excluded at this point (**Supplementary Table 1**). Automated reclustering was performed on all remaining samples to calibrate clusters on the study sample set.

Poor-quality assays were excluded before downstream quality-control processes by extensive manual review of clustering performance. A subset of good-quality SNPs was identified on the basis of the ranking of quality metrics: cluster separation (<0.4), signal intensity (<1.0), call rate (<0.98) and allele frequency. In addition, SNPs that mapped to the Y chromosome or mitochondria, were nonpolymorphic, were duplicates or zeroed in the default Illumina cluster file were also excluded. This resulted in a dataset of 165,549 good-quality SNPs (**Supplementary Table 2**).

To facilitate the meta-analysis and reduce differential missingness, each of the six population datasets was processed as a discrete entity. SNPs were excluded from each of the datasets with a call rate <0.99 (cases or controls), MAF < 0.01 or if they deviated from Hardy-Weinberg equilibrium (HWE) ($P_{HWE} < 5.7 \times 10^{-7}$). Samples were excluded with a call rate <0.99 or if they were identified as outliers on the basis of autosomal heterozygosity (**Supplementary Tables 3 and 4**). Samples were also excluded if they were considered to be outliers on the basis of ethnicity inferred by principal component analysis (PCA). PCA was performed using EIGENSOFT v4.2 with HapMap phase 2 samples as reference populations on a subset of SNPs with MAF > 0.05 and filtered to minimize intermarker LD (excluding the MHC region, 23 regions of high LD and previously confirmed rheumatoid arthritis susceptibility regions) (**Supplementary Fig. 1**). Cryptic relatedness was assessed within each dataset by calculating identity by descent using PLINK v1.07 and the PCA SNP set. A single sample from any related pair ($PI_HAT > 0.1875$) was removed from the analysis (informed by call rate). In addition, identity by descent was inferred across all six datasets to exclude cross-dataset related individuals (**Supplementary Table 5**). The genomic control inflation factor (λ_{GC}) was calculated within each Immunochip dataset using SNPs included as a deep replication for a study investigating the genetic basis for reading and writing ability. This set of SNPs was filtered as described for the PCA SNP set, leaving a total of 1,469 SNPs distributed evenly across the genome. The λ_{GC} for the datasets was estimated at 1.07 (UK), 1.03 (US), 0.97 (Sweden EIRA), 0.94 (Sweden Umea), 1.12 (The Netherlands) and 1.10 (Spain). Using the same SNPs to estimate λ_{GC1000} (where the factor is scaled to the equivalent of 1,000 cases and 1,000 controls) in the Immunochip meta-analysis resulted in a rescaled λ of 1.02 (or 1.23 without rescaling).

All newly identified loci remained significantly associated when including gender or λ_{GC} as a covariate in the analysis (**Supplementary Table 15**).

Immunochip meta-analysis. Association statistics were calculated in each dataset using logistic regression under an additive model (SNPs coded 0, 1 or 2 with respect to the minor allele dosage) and incorporating the top ten principal components as covariates. ORs and standard errors were combined across the six datasets using an inverse-variance meta-analysis and assuming a fixed effect.

Independent effects. Initial evidence for secondary effects was assessed at each of the previously known and newly identified loci using forward stepwise logistic regression. The index SNP at each region was included as a covariate, and the association statistics were recalculated for the remaining test SNPs. This process was repeated until no SNPs reached the minimum level of significance. The criteria for declaring an independent effect were defined as $P < 5 \times 10^{-4}$, not highly correlated with index SNP and a conditioned P value that was not substantially different from the unconditioned value. We next tested if the two-SNP model fitted the risk at the locus significantly better than the one-SNP model using a likelihood ratio test.

The effect estimates for each two-SNP haplotype were calculated by including indicator variables for the carriage of haplotypes. The indicator variables, constructed by phasing the genotype data for each region satisfying the above criteria, were phased using the SHAPEIT algorithm¹⁸.

GWAS meta-analysis. GWAS case-control collections were previously described¹. Six collections were included in the present study: BRASS, CANADA, EIRA, NARAC1, NARAC2 and WTCCC. After quality control and data filtering, the datasets were imputed using IMPUTE and haplotype-phased HapMap Phase 2 European CEU founders as a reference panel¹⁹.

We used identity-by-state (IBS) estimates to remove related samples across the Immunochip and GWAS collections using GWAS genotype data instead of imputed data. In each of the 12 collections, we selected a set of SNPs with a missing genotype rate <0.5%, MAF > 5% and $P_{HWE} > 5 \times 10^{-7}$. We then extracted SNPs that passed these filters and were shared between the 12 collections. After further LD pruning and resolving flipping issues, the data from the 12 collections were merged to calculate the IBS statistics. When related samples were identified (siblings or duplicates), the sample from the GWAS collection was removed to preferentially keep Immunochip data in the subsequent association analyses. Filtering and IBS calculations were performed using PLINK²⁰. Two GWAS datasets, EIRA and NARAC1, were excluded because of strong overlap (>90% of the rheumatoid arthritis cases) with the Immunochip Sweden EIRA and US collections, respectively. This resulted in a total sample size of 13,838 rheumatoid arthritis cases and 33,742 controls, distributed in ten collections (**Table 1**).

The software SNPTEST v2.2 was used to conduct a logistic regression analysis of rheumatoid arthritis case-control status in each GWAS collection, conditioning on the five first eigenvectors from the PCA analysis and after excluding SNPs with low statistical information (info score < 0.7) or MAF < 1%. We also excluded SNPs that were not represented in the filtered Immunochip data. The λ_{GC} values for the individual datasets were estimated at 1.04 (BRASS), 1.02 (CANADA), 1.04 (NARAC2) and 1.05 (WTCCC). There was a slight inflation in λ_{GC} in these cohorts when using the 1,469 SNPs included on Immunochip to investigate the genetic basis of reading and writing ability: 1.11 (BRASS), 1.15 (CANADA), 1.07 (NARAC2) and 1.05 (WTCCC).

We conducted an inverse-variance weighted meta-analysis to combine the results across the ten collections. We also computed Cochran's Q statistics and I^2 statistics to assess heterogeneity across collections. The meta-analysis and heterogeneity statistics computations were adapted from the MANTEL program²¹.

Serological subtype statistical analyses. Multinomial logistic regression was applied to compute ORs, 95% CIs and P values for association between the minor allele at every locus and either ACPA-positive ($OR_{ACPA\text{-positive}}$) or ACPA-negative rheumatoid arthritis ($OR_{ACPA\text{-negative}}$) assuming additivity on the log-odds scale (every locus was coded as 0, 1 or 2 corresponding to the copy number of the minor allele). The minor allele was defined according to the allele frequency in the total population, including cases and controls. To test for differences between $OR_{ACPA\text{-positive}}$ and $OR_{ACPA\text{-negative}}$, the linear combination $\beta_+ - \beta_-$, where β_+ is $\log(OR_{ACPA\text{-positive}})$ and β_- is $\log(OR_{ACPA\text{-negative}})$ was calculated, along with its standard error. This enables a P value for the difference in association to be calculated.

GRAIL analysis. We performed GRAIL analysis (<http://www.broadinstitute.org/mpg/grail/grail.php>) using HG18 and Dec2006 PubMed datasets, default settings and the 46 genome-wide significant rheumatoid arthritis susceptibility loci (most associated SNP) as seeds.

Interaction analysis. We performed an analysis of epistasis using the most significantly associated SNP from each of the 46 loci (Table 2). Logistic regression was performed in PLINK to model epistasis in each of the six datasets with the top ten principal components included as covariates. For each pair of SNPs, the likelihood ratio test was used to compute the *P* value of the interaction term for each dataset. Epistasis results were combined using METAL and were Bonferroni corrected.

eQTL analysis. eQTL analysis was done on the peripheral blood of 1,469 unrelated individuals (1,240 samples run on the Illumina HT12v3 platform and 229 samples run on the Illumina H8v2 platform) from the UK and The Netherlands. Details of the eQTL analysis have been previously described²². In short, we assessed the effect of all rheumatoid arthritis-associated SNPs (Table 2) on the expression of genes located within 250 kb to the left and right of the SNP (*cis* eQTLs).

All individuals from the eQTL study were genotyped on the Illumina Hap300K platform and then imputed to HapMap 2 using Impute 2.0 software. Because not all SNPs from the Illumina ImmunoChip platform were genotyped or imputed on the 1,469 eQTL samples, we used the following strategy (Supplementary Fig. 5). First, we investigated whether the SNP is present in the eQTL data and passed the quality control for eQTL mapping (MAF \geq 5%, $P_{\text{HWE}} \geq$ 0.001, call rate \geq 95%). From 50 rheumatoid arthritis SNPs, 26 were present in HapMap-imputed datasets and were directly assessed for eQTL effects (Supplementary Table 13). For the other 24 SNPs not present in our HapMap imputed data, we checked whether the rheumatoid arthritis SNP was available in the 1000 Genomes database. If so, we queried all SNPs within 10 Mb of the rheumatoid arthritis SNP that were also present in the eQTL data and would pass the eQTL quality control measures and picked the SNP with the highest LD that was present in HapMap after quality control.

The threshold of $r^2 > 0.8$ for the LD was used. For 12 SNPs, no proxy was available using our criteria, and these SNPs were not included in the eQTL analysis. For the remaining 12 SNPs, the best proxy SNP is included in the eQTL table (Supplementary Fig. 5).

We also performed a *cis*-eQTL analysis for the top associated gene expression probe, as well as two conditional analyses, one conditioning on the effect of the rheumatoid arthritis SNP (gSNP) and one conditioning on the effect of the top eQTL SNP (eSNP) (Supplementary Table 13).

The rheumatoid arthritis-associated SNP was labeled as having a primary effect on gene expression if it was either the top eQTL in the locus or was a good proxy for the top eQTL SNP ($r^2 > 8$). It was labeled as an independent eQTL if it showed an effect after conditioning on the primary eQTL. From 20 rheumatoid arthritis SNPs that showed an eQTL effect, 13 had either an independent or primary eQTL effect on one or more probes (22 SNP-probe combinations). A further seven SNPs were not significant after the conditioning of the strongest eQTL signal in the locus, suggesting that they are not primary eQTLs.

18. Delaneau, O., Marchini, J. & Zagury, J.F. A linear complexity phasing method for thousands of genomes. *Nat. Methods* **9**, 179–181 (2012).
19. Marchini, J., Howie, B., Myers, S., McVean, G. & Donnelly, P. A new multipoint method for genome-wide association studies by imputation of genotypes. *Nat. Genet.* **39**, 906–913 (2007).
20. Purcell, S. *et al.* PLINK: a tool set for whole-genome association and population-based linkage analyses. *Am. J. Hum. Genet.* **81**, 559–575 (2007).
21. de Bakker, P.I. *et al.* Practical aspects of imputation-driven meta-analysis of genome-wide association studies. *Hum. Mol. Genet.* **17**, R122–R128 (2008).
22. Fehrmann, R.S. *et al.* Trans-eQTLs reveal that independent genetic variants associated with a complex phenotype converge on intermediate genes, with a major role for the HLA. *PLoS Genet.* **7**, e1002197 (2011).